Supplementary Material

Metawaveguide for Asymmetric Interferometric Light-Light Switching

Han Zhao[1†], William S. Fegadolli[2†], Jiakai Yu[1†], Zhifeng Zhang[1], Li Ge[3], Axel Scherer[2] and Liang Feng[1*]

[1] *Department of Electrical Engineering, The State University of New York at Buffalo, Buffalo, NY 14260, USA*

[2]*Department of Physics and Kavli Nanoscience Institute, California Institute of Technology, Pasadena, CA 91125, USA*

[3]*Department of Engineering Science and Physics, College of Staten Island, CUNY, Staten Island, NY 10314, USA and The Graduate Center, CUNY, New York, NY 10016, USA*

[†]These authors contributed equally to this work.

*Email: fengl@buffalo.edu

1. Asymmetric inteferometric light-light switching with coherent perfect absorption (CPA)

Under the CPA condition ($M_{11}=0$), it is straightforward to show, based on the optical transfer matrix [Eq. (1)], that $M_{11}=t-r_L r_R/t$ in terms of the transmission coefficient t and reflection coefficients r_L, r_R, which means that $t=\sqrt{r_L r_R}$ is needed for CPA. Previous demonstrations of CPA[4,7,34] used systems with a mirror symmetry, and as a result, the control beam $B(L)$ has the same intensity as the signal beam $A(0)$. In other words, $|M_{21}|\equiv|r_L/t|=1$ in the previously studied systems, since $B(L)=M_{21}A(0)$ when there is no reflection or scattering ($A(L),B(0)=0$).

The goal we set to achieve, i.e., using a weak control beam $B(L)$ to bring a strong signal beam $A(0)$ into CPA, is satisfied when $M_{21} \ll 1$. It indicates that the reflection from the left should be much weaker than the transmission. Again combined with the CPA condition, we know that the transmission in turn must be much weaker than the reflection from the right. Therefore, we have identified a necessary requirement to achieve our goal, which is a strongly *asymmetric reflection*, i.e., $|r_L| < |r_R|$. We also note that CPA is sensitive to the relative phase of the control beam with respect to the signal beam: if we change the phase of $B(L)$ from $M_{21}A(0)$, then the intensity of the scattered light gradually increases from zero to a significant amount, the maximum of which is the "on" mode of our operation while CPA provides the "off" mode.

In our approach, we manipulate the spatial index-absorption modulation of a photonic waveguide in the vicinity of the exceptional point of the scattering matrix, defined by

$$S_c = \begin{pmatrix} t & r_L \\ r_R & t \end{pmatrix}.$$

The exceptional point occurs when the two scattering values $\sigma_\pm = \pm\sqrt{r_L r_R}$ of the scattering matrix become the same, which is usually achieved with a vanished r_L and a finite r_R or vice versa. This condition is the extreme limit of asymmetric reflection, which is required by an asymmetric CPA as mentioned above. However, if we were to achieve a CPA right at such an exceptional point, then the CPA condition $t = \sqrt{r_L r_R}$ mentioned previously requires that the transmission has to vanish as well (together with the other reflection coefficient). This is obviously not a useful situation to realize a switch, as $r_L = r_R = t = 0$ means that the device acts an optical blackhole no matter from which side it is illuminated or whether there is a control beam.

This obstacle is removed if we operate near the exceptional point instead, which still provides a strong asymmetric reflection while maintaining a finite transmission coefficient. We further note that we do not want to operate too close to the exceptional point, which would lead to a poor transmission ($t \approx 0$) and be not very useful for an energy-efficient device. Therefore, we choose to operate moderately far from the exceptional point while still keep a good intensity ratio between the control beam and the signal beam, which is 3 in the example given in the main text. As we show in the manuscript, this operating principle in a quasi-PT symmetric system provides a convenient platform to realize CPA with a weak controlling beam.

It is worth noting that the "on" and "off" modes here are defined by the eigenstates of the scattering matrix. Since our system is linear any input can be decomposed into these modes to calculate the scattered amplitudes.

2. Design of non-Hermitian modulations for asymmetric interferometric light-light switching.

Within the modulated region, the coupled mode equations between forward and backward propagating light are derived as

$$\frac{\mathrm{d}A(z)}{\mathrm{d}z} = iC_0\alpha A(z) + iC_1\kappa B(z)$$
$$\frac{\mathrm{d}B(z)}{\mathrm{d}z} = -iC_{-1}\kappa A(z) - iC_0\alpha B(z)$$

where $C_{-1} = (1-\delta)/8\delta$, $C_0 = -i/2\pi$, and $C_1 = (1+\delta)/8\delta$ are the corresponding Fourier coefficients, while α is the attenuation constant caused by the introduced absorption and κ is the coupling coefficient between forward and backward propagating modes. Then the transfer matrix M in Eq. (2) reads

$$M_{11} = \cosh(\eta L) + i\frac{C_0\alpha}{\eta}\sinh(\eta L) \qquad M_{12} = i\frac{C_1\kappa}{\eta}\sinh(\eta L)$$
$$M_{21} = -i\frac{C_{-1}\kappa}{\eta}\sinh(\eta L) \qquad M_{22} = \cosh(\eta L) - i\frac{C_0\alpha}{\eta}\sinh(\eta L),$$

where $\eta^2 = C_{-1}C_1\kappa^2 - C_0\alpha^2$. The CPA condition $M_{11} = 0$ in this case is equivalent to

$$\sinh(\eta L) = \frac{i\eta}{\kappa\sqrt{C_1C_{-1}}} \ , \ \cosh(\eta L) = \frac{\alpha C_0}{\kappa\sqrt{C_1C_{-1}}},$$

with the constraint $\cosh(\eta L)^2 - \sinh(\eta L)^2 = 1$ taken into consideration. We then find M_{21} is given by $\sqrt{C_{-1}/C_1} = \sqrt{(1-\delta)/(1+\delta)}$ in the CPA mode, and we denote it by $\sqrt{\xi}\exp(-i\varphi)$. Here ξ and φ are the intensity ratio of signal to control and the incident phase of the control (where we assume the incident phase of the signal is always 0), respectively. The intensity ratio of the signal beam and the control beam in the CPA mode is then given by $\xi = (1+\delta)/(1-\delta)$, with the total modulation length satisfying

$$L = \sinh^{-1}\left(\frac{8\delta\eta}{\kappa\sqrt{\delta^2 - 1}}\right)\Big/\eta \, .$$

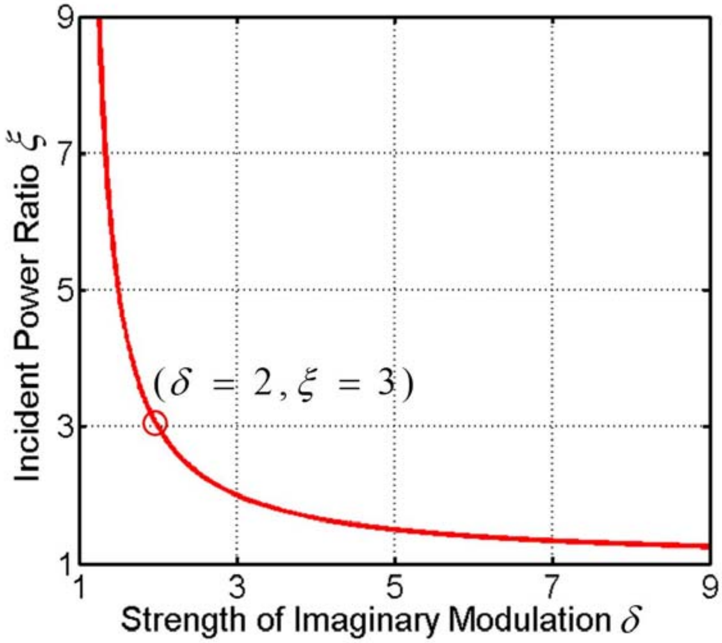

Fig. S1. Evolution of intensity ratio ξ (strong laser signal to weak control beam) in the CPA mode as function of the imaginary modulation depth δ. The red circle marks the parameter $\delta = 2, \xi = 3$ used in the experimental demonstration of asymmetric interferometric light-light switching.

Fig. S1 shows the dependence of intensity ratio ξ on the strength of imaginary modulation δ. It can be seen that approaching the exceptional point ($\delta = 1$) would allow the power ratio being infinitely large. In other words, one can bring a strong laser signal to the CPA state with an infinitesimally weak control beam by an appropriate phase control. In contrast, operating far away from the exceptional point will decrease the contrast of two input intensities and eventually result in the CPA mode with equally strong incidences, as demonstrated in the prior works. For experimental demonstration, we chose the incident power ratio contrast as $\xi = 3$, which necessarily corresponds to the modulation of $\delta = 2$.

3. Sample fabrication.

The fabrication starts with an SOI wafer. Periodically arranged sinusoidal shaped combo structures are first patterned in polymethyl methacrylate (PMMA) by electron beam lithography with accurate alignment, followed by electron beam evaporation of Ge/Cr and lift-off. Then the

Si waveguide with cosine shaped sidewall modulations is defined with aligned electron beam lithography using hydrogen silsesquioxane resist(HSQ), followed by dry etching with mixed gases of SF_6 and C_4F_8. Finally, plasma enhanced chemical vapor deposition is used to deposit the cladding of SiO_2 on the entire wafer.

4. Experimental evaluation of output scattering coefficients

To characterize the spectra of minimum and maximum output scattering coefficients, we used CCD camera to capture the scattered light from the four grating couplers in one field of view (Fig. 3a). First, light scattered from two input grating couplers (I_1 and I_2) was captured at minimum camera exposure time (100 µs). In our experiment, the input power of the signal beam entering the metawaveguide was estimated approximately 2.5 µW and the control power was approximately 0.8 µW. An exemplary image is shown in Fig. S2. Because of the low exposure time, the weaker output light scattered at two output grating couplers (O_1 and O_2) can hardly be detected.

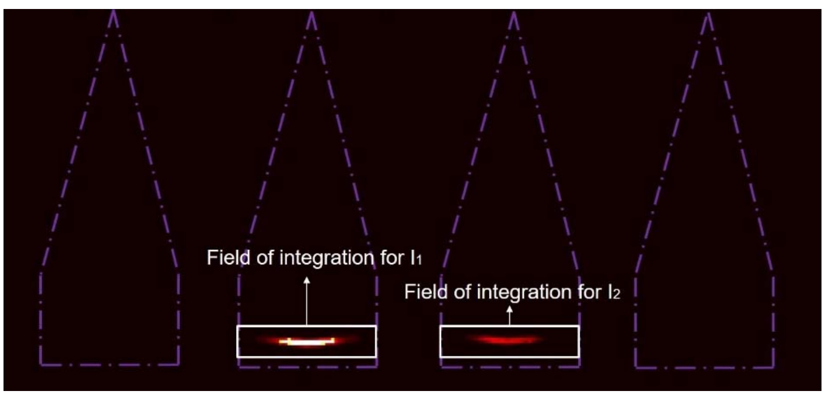

Fig. S2. Field of integration for measuring input signal-reference power at minimum camera exposure time of 100 µs. White rectangular zones are the areas of coupling gratings. In this box area, all the signals are summed to denote signal (left: I_1) and reference (right: I_2) inputs respectively. Dashed lines show the layout of silicon waveguide tapers and grating couplers.

Since light intensity is linearly proportional to the brightness value on captured image as long as no saturated exposure is reached on each pixel, the input signal and reference power can be estimated by integrating the pixels corresponding to their own coupling gratings. The field of integration in the characterization was circled as shown in Fig. S1. Therefore, the signal-to-reference input power ratio was determined by comparing the integrations of I_1 and I_2. By controlling the coupling efficiency from lensed fibers to on-chip waveguide ports, we tuned the signal-to-reference input power ratio at 3:1, consistent with the design.

When recording the total output intensity ((i.e. O_1 and O_2)), we increased the exposure time of the camera to 15 ms, such that the scattered light from output grating couplers could be clearly detected (see Fig. S3). At each wavelength, the phase difference between the signal and reference inputs was controlled by the optical delay line in free space. As the output intensity changed with respect to the phase difference, we captured images corresponding to minimum and maximum total output power. Fig. S3 showed the image of maximum output at the resonant wavelength (i.e. $\Delta = 0$), corresponding to the case in Fig. 3b. Here, the total outputs (O_1 and O_2) were obtained by integrating the light labeled in white boxes in Fig. S3, corresponding to the grating couplers. It is worth pointing out that the white boxes for integrating I_1, I_2, O_1, and O_2 in Figs. S2 and S3 are of the same size and the relative position to the corresponding grating coupler.

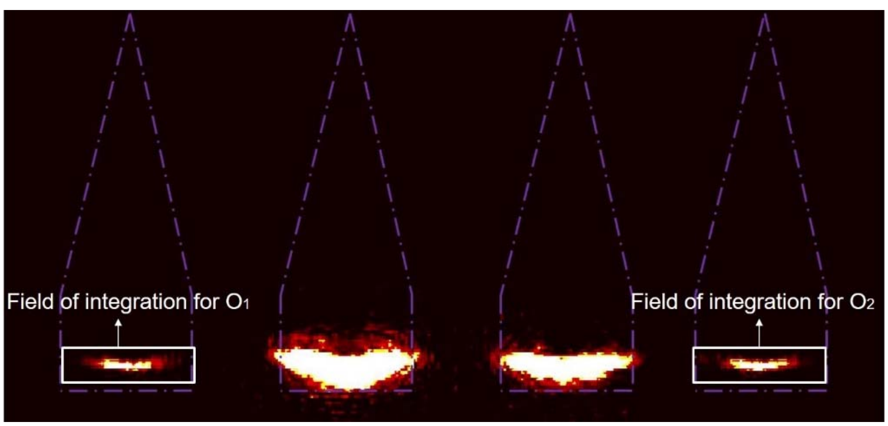

Fig. S3. Field of integration for measuring total output power at camera exposure time of 15 ms. White rectangular zones show the areas for integration corresponding to two output coupling gratings (O_1 and O_2). Dashed lines represent the layout of silicon waveguide taper and grating couplers.

Notice that the scattering light from I_1 and I_2 in Fig. S3 are already saturated and thus cannot accurately reflect the actual collected power. Therefore, to obtain the correct data for I_1 and I_2, we reduced the camera exposure time back to its minimum (100 μs), as shown in Fig. S2.

Since the value detected from the CCD camera increases linearly as the camera exposure time grows, the values of I_1 and I_2 corresponding to total input power were rescaled by multiplying 150, with respect to the maximum exposure time of 15 ms. The output scattering coefficients (Q_s) were then obtained using Eq. (3) with also considering the insertion loss from the directional couplers.

The observation of no scattering at output grating couplers at the CPA mode (Fig. S2) does not alter under the varied exposure time. However, with the wavelength detuning, the metawaveguide is away from the resonance. In such off-resonance conditions, the in-phase CPA condition cannot be reached and the two output grating couplers inevitably scatter some power even if they reached their minimum respectively [Figs. 4(b) and 4(c)]. In this regard, longer exposure time (if achievable) would reveal more apparent outputs at off-resonance, which is consistent with theoretical prediction.